

Synthesis and characterization of the titanium complexes bearing two β -enaminoketonato ligands with electron withdrawing groups/modified phenyls and their behaviors for ethylene (co-)polymerization†

Wei-Ping Ye, Xin-Cui Shi, Bai-Xiang Li, Jing-Yu Liu,* Yue-Sheng Li, Yan-Xiang Cheng and Ning-Hai Hu

Received 1st February 2010, Accepted 5th July 2010

DOI: 10.1039/c001987a

A series of new titanium complexes with two asymmetric bidentate β -enaminoketonato [N,O] ligands (**2b–t**), $[\text{PhN}=\text{C}(\text{CF}_3)\text{CHC}(\text{Ar})\text{O}]_2\text{TiCl}_2$ (**2b**, Ar = $-\text{C}_6\text{H}_4\text{F}(o)$; **2c**, Ar = $-\text{C}_6\text{H}_4\text{F}(m)$; **2d**, Ar = $-\text{C}_6\text{H}_4\text{F}(p)$; **2e**, Ar = $-\text{C}_6\text{H}_4\text{Cl}(p)$; **2f**, Ar = $-\text{C}_6\text{H}_4\text{OMe}(p)$; **2g**, Ar = $-\text{C}_6\text{H}_4\text{CF}_3(p)$; **2h**, Ar = $-\text{C}_6\text{H}_4\text{CF}_3(m)$; **2i**, Ar = $-\text{C}_6\text{H}_4\text{CF}_3(o)$; **2j**, Ar = $-\text{C}_6\text{H}_4\text{Cl}(o)$; **2k**, Ar = $-\text{C}_6\text{H}_4\text{Br}(o)$; **2l**, Ar = $-\text{C}_6\text{H}_4\text{I}(o)$; **2m**, Ar = $-\text{C}_6\text{H}_3\text{F}_2(2,4)$; **2n**, Ar = $-\text{C}_6\text{H}_3\text{F}_2(2,6)$; **2o**, Ar = $-\text{C}_6\text{H}_3\text{F}_2(3,4)$; **2p**, Ar = $-\text{C}_6\text{H}_3\text{F}_2(3,5)$; **2q**, Ar = $-\text{C}_6\text{F}_5$; **2r**, Ar = $\text{C}_6\text{F}_4\text{OMe}$; **2s**, Ar = $-\text{C}_6\text{H}_3\text{Cl}_2(2,6)$; **2t**, Ar = $-\text{C}_6\text{H}_3\text{Cl}_2(2,5)$), have been synthesized based on substituted acetophenones. X-Ray analyses reveal that complexes **2h**, **2k**, **2m**, and **2n** adopt distorted octahedral geometry around the titanium center, in which the two chloride ligands are situated in the *cis*-orientation. **2s** also adopts distorted octahedral geometry, but the two chloride ligands in it are situated in the *trans*-orientation due to the increase of the steric effect of the phenyl derived from the acetophenone. The influence of the substituent effects on catalyst performance, including catalytic activities and the molecular weight distribution of the polymers obtained, was investigated in detail. With modified methylaluminoxane (MMAO) as a cocatalyst, complexes **2b–r** and **2t** are active catalysts for ethylene polymerization at room temperature, and produce high molecular weight polymers. It is observed that the catalytic activities are significantly enhanced by introducing some electron-withdrawing groups, such as $-\text{F}$, $-\text{Cl}$ and $-\text{CF}_3$, into the suitable positions of the phenyl ring close to the oxygen donor. It should be noted that complexes **2c–i**, **2p**, **2n** and **2t** are also capable of promoting the living copolymerization of ethylene with norbornene at room temperature, yielding high molecular weight copolymers with narrow molecular weight distributions (PDI = 1.05–1.30).

Introduction

In the last decade, a significant amount of research has focused on the development of non-metallocene catalysts for olefin polymerization.^{1–24} To optimize catalyst performance and polymer properties, different catalytic systems have been investigated, resulting in the discovery of a number of highly active catalysts such as group 4 transition metal complexes^{2–8} and late transition metal complexes.^{9–14} Especially in recent years, Fujita, Coates, and Pellecchia have developed a class of titanium catalysts bearing phenoxy-imine ligands (named FI Catalysts) for olefin polymerizations.^{15–17} Introducing heteroatom(s) and/or heteroatom-containing substituent(s) in the ligand have led to the discovery of a new series of FI Catalysts having fluorine atom(s) in the ligand that display unprecedented catalytic performance for the living polymerization of ethylene.^{15,16} Subsequently, Coates and coworkers reported a facile synthesis of new titanium catalysts containing ancillary non-fluorinated phenoxyketimine ligand of type, $(\text{Phi-R})_2\text{TiCl}_2$ for the living ethylene polymerization.¹⁸ These results suggested that variation of the ligand structure may lead to profound changes in the catalytic activity and the properties of the polymer.

State Key Laboratory of Polymer Physics and Chemistry, Changchun Institute of Applied Chemistry, Chinese Academy of Sciences, Changchun, 130022, China. E-mail: lly@ciac.jl.cn; Fax: +86-431-85262039

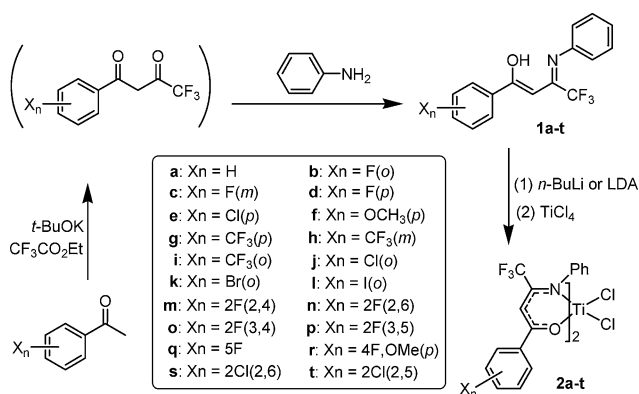
† Electronic supplementary information (ESI) available: Additional experimental details. CCDC reference numbers 763881–763884 and 763886. For ESI and crystallographic data in CIF or other electronic format see DOI: 10.1039/c001987a

We are interested in the design and synthesis of efficient transition metal catalysts for precise, controlled olefin polymerization. Previously, we reported the type of titanium catalysts chelating asymmetrical bidentate β -enaminoketonato ligands, $[\text{ArN}=\text{C}(\text{R}_1)\text{CHC}(\text{R}_2)\text{O}]_2\text{TiCl}_2$, and their use as catalyst precursors for olefin polymerization.^{19–23} Both steric and electronic effects in the R_1 and R_2 groups showed greatly influence on the polymerization performance.^{19,20,22} The trifluoromethyl group in the β -enaminoketonato ligands (R_1) appears to be required for the generation of high activity. Due to the fact that complex **2a** ($\text{R}_1 = \text{CF}_3$, $\text{R}_2 = \text{Ph}$) exhibited living characteristics for ethylene polymerization and ethylene/norbornene or other monomer copolymerization,^{19,21} we therefore decided to extend the study by introducing some substituents into the phenyl ring located in R_2 moiety and investigate the relationship between substituent effects and catalytic performances. In this paper, we present the synthesis and characterization of a series of new titanium complexes of the type $[\text{ArN}=\text{C}(\text{CF}_3)\text{CHC}(\text{R}_2)\text{O}]_2\text{TiCl}_2$, as well as their behavior towards ethylene and ethylene/norbornene copolymerization in the presence of MMAO.

Results and discussion

Synthesis and characterization of new titanium complexes

The titanium complexes **2b–t** were synthesized according to the reaction sequence shown in Scheme 1.^{20–22} A tandem sequence of



Scheme 1 General synthetic route of the titanium complexes used in this study.

Claisen condensation between acetophenone derivatives and ethyl trifluoroacetate and the condensation of the resulted β -diketone with aniline in the acidic toluene was used to synthesize these new β -enaminoketonates ligands **1b–t**. Treatment of TiCl_4 with two equivalents of the lithium salts of **1b–t** in dry diethylether gave **2b–t** in moderate to high yields. It is noticed that in the process of the synthesis of complexes **2k**, **2i** and **2q**, we chose lithium diisopropylamide (LDA) as the base instead of $n\text{-BuLi}$ to avoid possible side reactions, such as halogen–lithium exchange and nucleophilic substitution.^{25,26} The resultant complexes were obtained as deep red or black crystalline solids.

The molecular structures of complexes **2h**, **2k**, **2m**, **2n** and **2s** were confirmed by X-ray crystal analysis. The crystals suitable for X-ray diffraction were grown from dichloromethane–hexane solutions. The crystallographic data together with the collection and refinement parameters are summarized in Table 1. The molecular structures of these complexes are shown in Fig. 1–5, respectively, and the selected bond lengths and bond angles are summarized in Table 2.

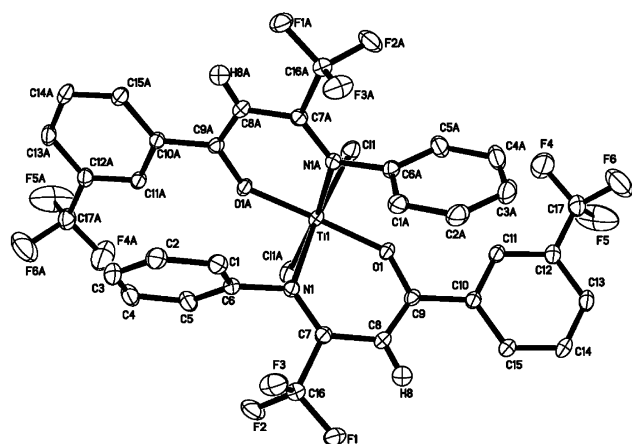


Fig. 1 Molecular structure of complex **2h** with thermal ellipsoids at 30% probability level. Hydrogen atoms (except H8 and H8A) are omitted for clarity.

In the solid state, compound **2h**, which has a CF_3 group on the *meta* position of the phenyl ring, adopts a distorted octahedral geometry around the titanium center with *trans* oxygen atoms, *cis* nitrogen atoms and *cis* chlorine atoms, which is the same as the case

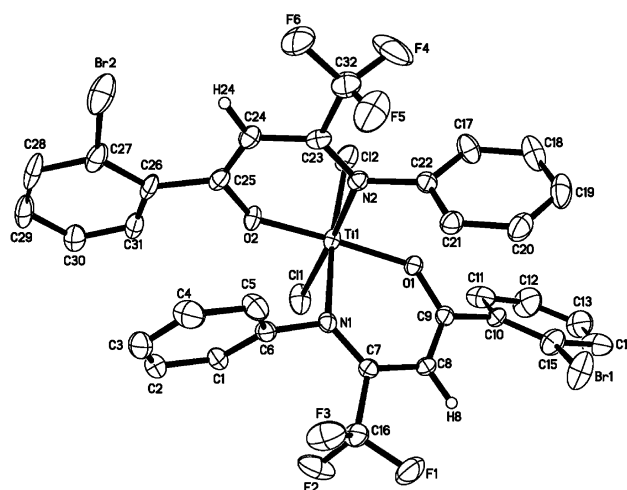


Fig. 2 Molecular structure of complex **2k** with thermal ellipsoids at 30% probability level. Hydrogen atoms (except H8 and H24) are omitted for clarity.

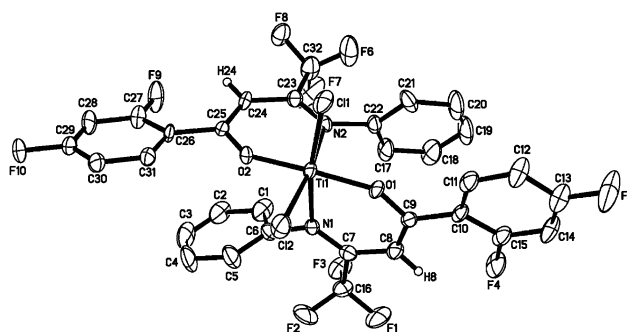


Fig. 3 Molecular structure of complex **2m** with thermal ellipsoids at 30% probability level. Hydrogen atoms (except H8 and H24) are omitted for clarity.

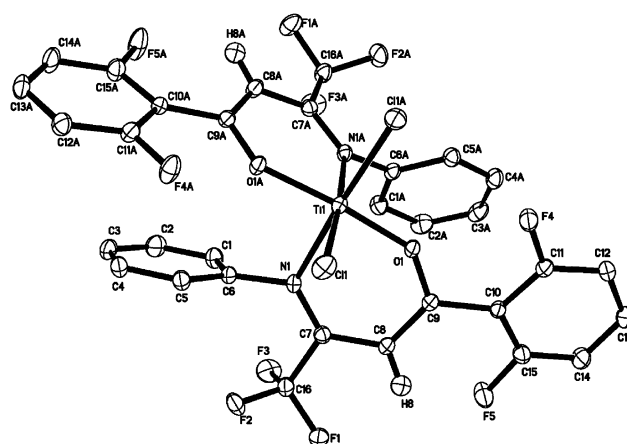


Fig. 4 Molecular structure of complex **2n** with thermal ellipsoids at 30% probability level. Hydrogen atoms (except H8 and H8A) are omitted for clarity.

reported for complex **2a**.¹⁹ All of the bond distances and angles around the titanium center of **2h** are very close to the values of **2a** (**2h**: $\text{Ti–O} = 1.879(15)$ Å, $\text{Ti–N} = 2.207(2)$ Å, $\text{Ti–Cl} = 2.274(8)$ Å, $\text{O–Ti–O} = 166.63(11)^\circ$, $\text{Cl–Ti–Cl} = 96.64(5)^\circ$, $\text{N–Ti–N} = 89.34(10)^\circ$;

Table 1 Crystal data and structure refinements of complexes **2h**, **2k**, **2m**, **2n** and **2s**

	2h	2k	2m	2n	2s
Empirical formula	C ₃₄ H ₂₀ Cl ₂ F ₁₂ N ₂ O ₂ Ti	C ₃₂ H ₂₀ Br ₂ Cl ₂ F ₆ N ₂ O ₂ Ti	C ₃₂ H ₁₈ Cl ₂ F ₁₀ N ₂ O ₂ Ti	C ₃₂ H ₁₈ Cl ₂ F ₁₀ N ₂ O ₂ Ti	C ₃₂ H ₁₈ Cl ₆ F ₆ N ₂ O ₂ Ti
Formula weight	835.32	857.12	771.28	771.28	837.08
Crystal system	Monoclinic	Monoclinic	Monoclinic	Monoclinic	Orthorhombic
Space group	<i>P2</i> / <i>n</i>	<i>P2</i> ₁ / <i>n</i>	<i>P2</i> ₁ / <i>n</i>	<i>C2</i> / <i>c</i>	<i>Pbca</i>
<i>a</i> /Å	11.8417(9)	11.2111(10)	18.949(7)	21.721(2)	10.9398(6)
<i>b</i> /Å	8.2093(6)	15.5277(14)	8.403(3)	8.4944(8)	13.7340(8)
<i>c</i> /Å	17.3695(12)	19.3685(17)	20.493(7)	19.0168(17)	22.5112(13)
α /°	90.00	90.00	90.00	90.00	90.00
β /°	93.1170(10)	102.674(2)	100.738(5)	118.4900(10)	90.00
γ /°	90.00	90.00	90.00	90.00	90.00
<i>V</i> /Å ³	1686.0(2)	3289.6(5)	3206(2)	3083.8(5)	3382.2(3)
<i>Z</i>	2	4	4	4	4
Density _{calcd} (Mg m ⁻³)	1.645	1.731	1.598	1.661	1.644
Absorption coefficient/mm ⁻¹	0.515	2.919	0.526	0.547	0.795
<i>F</i> (000)	836	1688	1544	1544	1672
Crystal size/mm	0.40 × 0.17 × 0.06	0.21 × 0.18 × 0.10	0.31 × 0.18 × 0.16	0.37 × 0.15 × 0.11	0.29 × 0.18 × 0.08
θ range for data collection (°)	2.03 to 25.68	1.70 to 25.03	1.62 to 25.03	2.13 to 26.03	1.81 to 25.35
Reflections collected	8793	16 828	15 682	8403	16 839
Independent reflections	3185 (<i>R</i> _{int} = 0.0200)	5809 (<i>R</i> _{int} = 0.0482)	5619 (<i>R</i> _{int} = 0.0508)	3035 (<i>R</i> _{int} = 0.0204)	3097 (<i>R</i> _{int} = 0.0200)
Data/restraints/parameters	3185/0/240	5809/12/418	5619/22/430	3035/0/222	3097/0/223
Goodness-of-fit on <i>F</i> ²	1.032	1.099	1.147	1.052	1.053
Final <i>R</i> indices [<i>I</i> > 2 σ (<i>I</i>)]: <i>R</i> ₁ , <i>wR</i> ₂	0.0444, 0.1130	0.0874, 0.2359	0.1302, 0.2938	0.0325, 0.0827	0.0451, 0.1188
Largest diff. Peak and hole/e Å ⁻³	0.835 and -0.367	4.761 and -0.983	1.862 and -0.967	0.290 and -0.291	1.154 and -0.706
Measurement <i>T</i> /K	185(2)	185(2)	185(2)	185(2)	187(2)

Table 2 Selected bond lengths (Å) and angles (°) for complexes **2h**, **2k**, **2m**, **2n** and **2s**

	2h	2k	2m	2n	2s
Ti–O (1)	1.8793(15)	1.889(5)	1.871(6)	1.8738(12)	1.8937(18)
Ti–O (1A or 2)	1.8793(15)	1.859(5)	1.865(6)	1.8738(12)	1.8937(18)
Ti–N (1)	2.207(2)	2.221(7)	2.207(8)	2.2241(15)	2.145(2)
Ti–N (1A or 2)	2.207(2)	2.180(7)	2.225(8)	2.2241(15)	2.145(2)
Ti–Cl (1)	2.2738(8)	2.261(3)	2.248(3)	2.2716(6)	2.2995(7)
Ti–Cl (1A or 2)	2.2738(8)	2.282(3)	2.284(3)	2.2716(6)	2.2995(7)
N (1)–Ti–N (1A or 2)	89.34(10)	87.8(2)	83.3(3)	89.37(7)	180.00(1)
O (1)–Ti–O (1A or 2)	166.63(11)	167.3(3)	168.6(3)	162.98(8)	180.00(1)
Cl (1)–Ti–Cl (1A or 2)	96.64(5)	97.11(11)	98.34(14)	96.35(3)	180.0
N (1)–Ti–O (1)	81.20(7)	82.0(2)	80.1(3)	80.95(5)	84.34(8)
N (1)–Ti–O (1A or 2)	89.27(7)	88.1(3)	90.4(3)	86.95(5)	95.66(8)
N (1)–Ti–Cl (1)	87.35(5)	87.88(19)	166.9(2)	175.19(4)	90.51(6)

2a: Ti–O = 1.874(18) Å, Ti–N = 2.209(2) Å, Ti–Cl = 2.270(11) Å, O–Ti–O = 166.25(13)°, Cl–Ti–Cl = 95.996(6)°, N–Ti–N = 88.74(12)°. Complexes **2k**, **2m**, **2n** and **2s**, with substituent(s) on the *ortho* position of the phenyl, show similar structures in the solid state. For complexes **2k** (Ar = *o*-BrPh), **2m** (Ar = 2,4-2FPh) and **2n** (Ar = 2,6-2FPh), the two oxygen atoms are situated in the *trans* position, while the two nitrogen atoms are in the *cis* position to each other, and so do the two chlorine atoms around the central titanium metal. However, all of these *trans* angles about the Ti atom in **2s** are constrained to 180° because the Ti atom lies on a crystallographic center of symmetry. Complex **2s** displays longer Ti–Cl and Ti–O bond distances of 2.2995(7) and 1.8937(18) Å, respectively, and shorter Ti–N bond distance of 2.145(2) Å than complex **2k** (Ti–Cl(1) = 2.261(3), Ti–O(1) = 1.889(5), Ti–N(1) = 2.221(7) Å).

It was interesting to note that there is overlapping of the phenyl ring located in the R₂ moiety in the crystal structure of complexes **2k**, **2m** and **2n**, indicating there is π – π stacking interactions between them. The geometrical parameters of the stacking contacts are as follows: the centroid–centroid distance

(*d*_{c–c}) is 4.346 Å (**2k**), 4.064 Å (**2m**) and 3.699 Å (**2n**). The interplanar distance (*d* _{π – π}) is 3.581 Å (**2k**), 3.528 Å (**2m**) and 3.414 Å (**2n**). The dihedral angle between ring planes is zero in the crystal structures of the three complexes.

As shown in Table 3, the distances between *ortho*-substituted fluorine atom and the olefinic proton are only 2.18/2.185 Å (**2m**) and 2.116 Å (**2n**), suggesting the existence of weak intramolecular hydrogen bonding interactions between these atoms.²⁷ The intermolecular interactions (π – π stacking) and the intramolecular interactions (hydrogen bonding) result in the small torsion angles (the torsion angle is the angle between the plane of β -enaminoketonato and the substituted phenyl ring) the small torsion angles in **2m** (8.99°, 13.59°) and **2n** (13.23°). An obvious difference in torsion angles for **2k** was seen not only because the N-aryl ring of the ligand is asymmetric, but also because the π – π stacking interactions just occur in the one side of the crystal structure. No π – π stacking interactions are observed in complexes **2a** and **2s**, and the hydrogen bonding interaction in **2s** is very weak as indicated by the distance (3.166 Å) of Cl(2)–H(8). From Table 3, we can also see that **2s** has a larger torsion

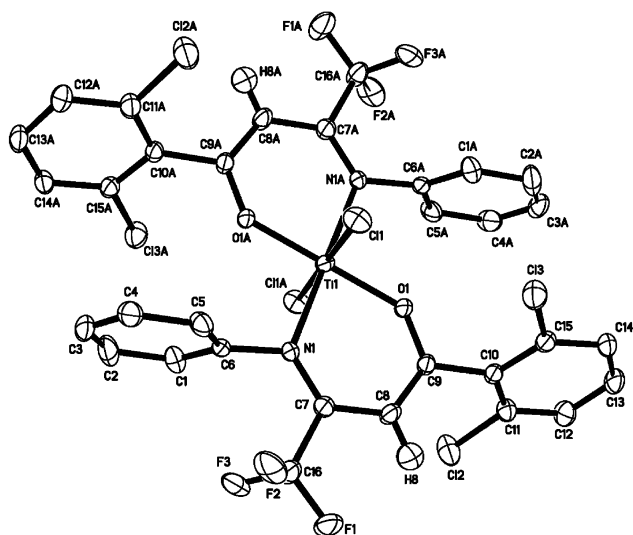


Fig. 5 Molecular structure of complex **2s** with thermal ellipsoids at 30% probability level. Hydrogen atoms (except H8 and H8A) are omitted for clarity.

Table 3 Distances between *ortho*-substituted halogen atom and olefinic proton (Å) and torsion angles (°) for complexes **2a**, **2k**, **2m**, **2n** and **2s**

	2a	2k	2m	2n	2s
Distances between <i>ortho</i> -substituted halogen atom and olefinic proton/Å					
F(4)–H(8)			2.180		
F(9)–H(24)			2.185		
F(5)–H(8)				2.116	
Br(1)–H(8)		2.824			
Br(2)–H(24)		2.512			
Cl(2)–H(8)					3.116
Torsion angles (°)					
C(8)–C(9)–C(10)–C(15)	11.17	49.26	8.99	13.23	65.14
C(24)–C(25)–C(26)–C(27)		8.78	13.59		

angle than **2a** (**2s**, 65.14°; **2a**, 11.17°), which is caused by bulkier substituents on the *ortho* position of the N-aryl ring. These facts indicate the intermolecular interaction (π - π stacking) and the intramolecular interaction (hydrogen bonding) can be considered as the determining factor for the association of molecules in the solid state.²⁷

Ethylene polymerization catalyzed by new titanium complexes

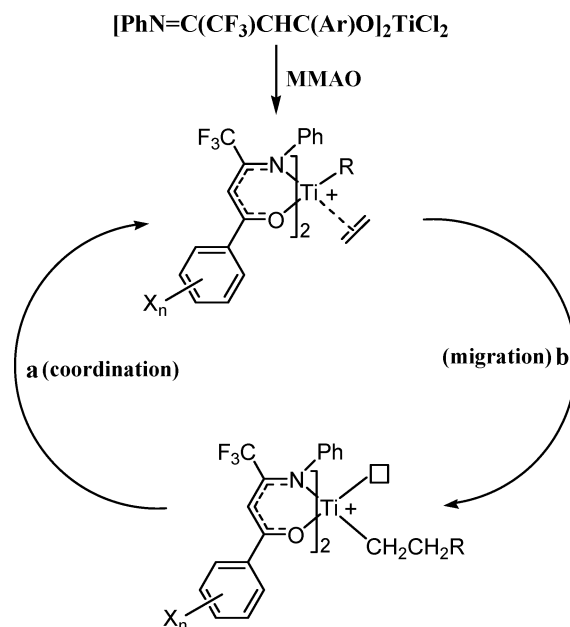
With MMAO as a cocatalyst, these new titanium complexes have been investigated as catalyst precursors for ethylene polymerization at room temperature under atmospheric pressure. The introduction of an electron-withdrawing group (EWG) and an electron-donating group (EDG) into the N-aryl moiety significantly affects catalytic activity and the properties of the resultant polymers, as shown in Table 4. The melting points, which range from 135–140 °C, and the ¹³C NMR data for the polymer products are consistent with linear polyethylene.

It is well-known that the ethylene polymerization by titanium catalyst can be described as “coordination-migration” mechanism like that shown in Scheme 2.²⁸ The progress of polymerization can be divided into two steps: “step a” (coordination of ethylene to center metal) and “step b” (migration of ethylene to metal–carbon

Table 4 Polymerization of ethylene by complexes **2a–t** activated with MMAO.^a

Entry	Catalyst/ μmol	Polymer/g	Activity ^b	<i>T</i> _m ^c /°C	<i>M</i> _n ^d /kg mol ⁻¹	<i>M</i> _w / <i>M</i> _n ^d
1	2a (1.0) ^{ref}	0.11	1.32	134	61.0	1.27
2	2b (1.0)	0.20	2.40	138	80.0	1.66
3	2c (1.0)	0.16	1.94	140	95.0	1.33
4	2d (1.0)	0.061	0.737	138	48.0	1.25
5	2e (1.0)	0.095	1.14	137	62.0	1.27
6	2f (1.0)	0.029	0.349	141	34.0	1.20
7	2g (1.0)	0.15	1.80	138	94.0	1.76
8	2h (1.0)	0.24	2.88	139	137	1.39
9	2i (1.0)	0.21	2.52	139	77.0	2.09
10	2j (1.0)	0.27	3.24	135	98.0	1.72
11	2k (1.0)	0.27	3.24	137	113	2.12
12	2l (1.0)	0.26	3.12	140	99.0	1.86
13	2m (1.0)	0.13	1.56	136	90.0	1.35
14	2n (1.0)	0.34	4.08	135	153	1.74
15	2o (1.0)	0.11	1.32	135	71.0	1.30
16	2p (1.0)	0.21	2.52	135	105	1.80
17	2q (1.0)	0.15	1.80	138	70.0	2.66
18	2r (1.0)	0.47	5.64	139	61.0	1.80
19	2s (10.0)	trace	—	—	—	—
20	2t (1.0)	0.40	4.80	134	131	2.04

^a Reaction conditions: 1 atm ethylene pressure, Al/Ti (mol ratio) = 2000, toluene 50 mL, polymerization for 5 min, the results shown for each entry are representative of at least three reproducible runs. ^b kg of PE/mmole_{Ti}·h. ^c Melting temperature measured by DSC. ^d Number-average molecular weight and polydispersity indexes of the resultant polyethylene determined by GPC using polystyrene standard.



Scheme 2 Potential mechanism of ethylene polymerization by the titanium complex.

bond), and the catalytic activity is determined by the rate of both steps as well as some kind of balance between them. Introduction of an EWG into the phenyl ring close to the oxygen donor makes ethylene coordinate to the titanium much easily, which can accelerate “step a”. For fluorine-containing phenyl, the role of the withdrawing inductive effect against donating conjugative effect depends on the F-position. The inductive effect which favors ethylene insertion is usually stronger than the conjugating effect

Table 5 Copolymerization of ethylene/norbornene by complexes **2a–t** activated with MMAO.^a

Entry	Catalyst/ μmol	Polymer/g	Activity ^b	NB Incorp. (mol%)	$T_g^c/^\circ\text{C}$	$M_n^d/\text{kg mol}^{-1}$	M_w/M_n^d
1	2a	0.860	1.72	44.3	121	340	1.17
2	2c	0.806	1.61	45.3	124	297	1.25
3	2d	0.641	1.28	39.4	115	224	1.09
4	2e	0.755	1.52	42.1	118	256	1.14
5	2f	0.157	0.313	46.7	132	51.3	1.07
6	2g	0.468	0.940	41.9	119	152	1.21
7	2h	0.837	1.67	46.9	130	289	1.19
8	2i	0.366	0.73	44.8	126	29.2	1.24
9	2p	0.494	0.99	40.2	115	167	1.28
10	2n	1.39	2.78	47.1	135	480	1.10
11	2t	0.567	1.13	45.3	130	185	1.21

^a Conditions: 3 μmol complex, 0.2 mol L⁻¹ concentration of the norbornene, Al/Ti molar ratio = 2000:1, $V_{\text{total}} = 50$ mL, atmospheric pressure, 25 $^\circ\text{C}$ polymerization for 10 min, the results shown for each entry are representative of at least two reproducible runs. ^b Activity in kg of polymer/ $\text{mmol}_{\text{Ti}}\cdot\text{h}$. ^c Number-average molecular weight and polydispersity index determined by GPC using polystyrene standard.

in *o*-F and/or *m*-F-containing phenyl.²⁹ Therefore, compared with **2a**, **2b** and **2c** exhibited relatively high catalytic activity. Contrarily, complex **2d** with the *p*-F in phenyl ring displayed low catalytic activity for ethylene polymerization due to the existence of strong conjugating effect.

In order to clarify the effect of a *para*-substituted group in the phenyl ring on the catalytic performance, complexes **2e** with a *p*-Cl, **2f** with a *p*-OMe and **2g** with a *p*-CF₃ were synthesized. As expected, **2e** and **2g** showed higher catalytic activity (1.14 and 1.80 kg mmol⁻¹_{Ti}·h bar, respectively), while **2f** exhibited much lower catalytic activity (0.349 kg mmol⁻¹_{Ti}·h bar) than **2a**. These results support the assumption that the low catalytic activities of **2d** results from the conjugating effect of *para*-substituted fluorine atom. It is worth noting that the polydispersity index ($M_w/M_n = 1.20$) of the polymer obtained by **2f** is obviously lower than that by **2a**, which implies that the electron-donating effect of the *para*-substituted group can suppress β -H chain transfer and produces a narrower polymer MWD. In addition, both **2h** with *m*-CF₃ and **2i** with *o*-CF₃ displayed high catalytic activities under the same conditions (2.88 and 2.52 kg mmol⁻¹_{Ti}·h bar, respectively). Moreover, complexes **2j–l** showed notable catalytic activities for ethylene polymerization (**2j**, 3.24; **2k**, 3.24; **2l**, 3.12 kg mmol⁻¹_{Ti}·h bar). These results suggested the existence of an electron-withdrawing group on the *ortho*- and/or *meta*-substituted phenyl ring is a necessary factor to improve the catalyst performance.

Complexes **2m–p** containing two fluorine atoms in the phenyl of the ligands were also synthesized. Complexes **2m** (2,4-2F) and **2o** (3,4-2F) exhibited comparable catalytic activities (**2m**, 1.56; **2o**, 1.32 kg mmol⁻¹_{Ti}·h bar) with **2a**. A significant increase in catalytic activity was observed if **2n** (2,6-2F) and **2p** (3,5-2F) was used (**2n**, 4.08; **2p**, 2.52 kg mmol⁻¹_{Ti}·h bar). Obviously, the degenerating effect of *para*-substituted fluorine atom counteracts the improving function of the *ortho*- or *meta*-substituted one towards catalytic performance. In order to further enhance the catalytic activity of titanium complex $[\text{PhN}=\text{C}(\text{CF}_3)\text{CHC}(\text{Ar})\text{O}]_2\text{TiCl}_2$, **2q** and **2r** were prepared and investigated for ethylene polymerization. Complex **2q** did not display surprising catalytic activity and produced the polymer with broader MWD (1.80 kg mmol⁻¹_{Ti}·h bar, $M_w/M_n = 2.66$, entry 17). However, **2r** showed the highest catalytic activity (5.64 kg mmol⁻¹_{Ti}·h bar, entry 18) among all the bis(β -enaminoketonato) titanium complexes studied here.

Introducing an extra chlorine atom in the phenyl of the ligands also significantly influenced the catalyst behaviors. Complex **2s** is inactive for ethylene polymerization due to the *trans* arrangement of the two chloride ligands (see Fig. 5), but **2t** (2,5-2Cl) exhibits higher catalytic activity (4.80 kg mmol⁻¹_{Ti}·h bar, entry 20) than **2j** (*o*-Cl).

Ethylene/norbornene copolymerization by the new titanium complexes

Ethylene/norbornene copolymers are important in various fields due to their remarkable material properties (*e.g.*, high thermal stability, high transparency, and high refractive indices). In our previous study, complex **2a** showed high activity for living ethylene/norbornene copolymerization.^{12a} Herein, we thus explored ethylene/norbornene copolymerization by some representative complexes. The typical results are summarized in Table 5. It should be noted that complexes **2c–i**, **2p**, **2n** and **2t** are also capable of promoting the living copolymerization of ethylene with norbornene at room temperature, yielding high molecular weight copolymers with narrow molecular weight distributions (PDI = 1.05–1.30). These results indicated that the presence of norbornene in the reaction medium and/or in the polymer chain seems beneficial for suppressing the chain termination or transfer.³⁰ Complex **2c** may be best suited as the catalyst precursor for this copolymerization in terms of exhibiting a high catalytic activity with efficient norbornene incorporation.

Conclusions

A series of new titanium complexes (**2b–t**) bearing two β -enaminoketonato ligands with electron-withdrawing or electron-donating group(s) have been synthesized and characterized. In the solid state, complexes **2h**, **2k**, **2m**, **2n** and **2s** adopt distorted octahedral geometry around the titanium center. Complexes **2h**, **2k**, **2m** and **2n** display *cis*-configuration of the two chlorine atoms around the titanium center, while complex **2s** showed *trans*-configuration of the two Ti–Cl bonds due to the steric effect of the two *ortho*-substituted chlorine atoms on the phenyl close to the oxygen donor. With MMAO as a cocatalyst, all the titanium complexes, except for **2s**, provide suitable

precatalysts for ethylene polymerization, and produce high molecular weight polymers with linear structures. Catalytic activity and polymer properties are influenced significantly by the structure of the β -enaminoketonato ligand. Both the electronic effect (including conjugative and inductive effect) and the position of the substituent on the ligand considerably influences the polymerization behavior of the titanium complexes. *Ortho*- and/or *meta*-halogenating considerably enhances the catalytic activity of $[\text{PhN}=\text{C}(\text{CF}_3)\text{CHC}(\text{Ar})\text{O}]_2\text{TiCl}_2$, but *para*-halogenating reduces the catalytic activity for ethylene polymerization. Complexes **2c–f**, **2m** and **2o** produce high molecular weight polyethylenes with relative narrow molecular weight distributions ($M_w/M_n = 1.20–1.35$), which implies the electron-donating group(s) are beneficial to obtaining the polymers with narrow MWD. In addition, the representative substituted complexes are also capable of promoting the living copolymerization of ethylene with norbornene at room temperature to produce high molecular weight copolymers with narrow molecular weight distributions ($M_w/M_n = 1.05–1.30$).

Experimental

All air and moisture-sensitive compounds were manipulated using standard Schlenk techniques or in a glove box under an argon atmosphere. The NMR data of the ligands and the complexes were obtained on a Bruker 300 MHz spectrometer at ambient temperature with CDCl_3 as a solvent (dried by MS 4 \AA). The NMR data of the copolymers were obtained on a Varian Unity 400-MHz spectrometer at 125 °C with $o\text{-C}_6\text{D}_4\text{Cl}_2$. Elemental analysis was performed on a Perkin-Elmer Series II CHN/O analyzer 2400. The DSC measurements were performed on a Perkin-Elmer Pyris 1 differential scanning calorimeter at a rate of 10 °C min^{-1} . The number-average molecular weights (M_n) and polydispersity indices (PDI) of the polymers were determined in 1,2,4-trichlorobenzene at 150 °C on a high temperature GPC using PL-GPC 220 instrument equipped with three PLgel 10 μm mixed-B LS columns.

Dried diethyl ether, hexane and toluene were purified from an MBraun SPS system. The ethyl trifluoroacetate, potassium *t*-butoxide, aniline and most of the acetophenone derivatives for ligands synthesis were purchased from Aldrich Chemical or Alfa Aesar Organics, and used without further purification. 2,3,5,6-Tetrafluoro-4-methoxyacetophenone was prepared according to the methods described in the literature.²⁴ Commercial titanium tetrachloride was distilled prior to use. The 1.6 M *n*-butyllithium solution in hexane was purchased from Acros. Modified methylaluminoxane (MMAO, 7% aluminium in heptane solution) was purchased from Akzo Nobel Chemical Inc. Commercial ethylene was directly used for polymerization without further purification. Complex **2a** was synthesized according to the procedure reported previously.

$\text{PhN}=\text{C}(\text{CF}_3)\text{CHC}(o\text{-FPh})\text{OH}$ (**1b**)

Ethyl trifluoroacetate (7.2 mL, 60 mmol) in ether (30 mL) was added dropwise to a stirred suspension of *t*-BuOK (5.4 g, 48 mmol) in dried ether (60 mL). The solution was stirred for 45 min at room temperature. A solution of 2'-chloroacetophenone (5.2 mL, 40 mmol) in ether (30 mL) was added, and the solution was stirred overnight. The reaction mixture was poured into a saturated

ammonium chloride solution, and then extracted with ether. The combined organic layer was washed with brine, dried over anhydrous sodium sulfate, filtered, and evaporated under reduced pressure to afford a deep yellow oil. To a stirred solution of this crude product in toluene (50 mL) were added aniline (5.6 mL, 60 mmol) and *p*-toluenesulfonic acid (*ca.* 20 mg) as a catalyst at room temperature. The mixture was heated and refluxed, and the water formed was removed azeotropically using a Dean–Stark apparatus for 24 h. During the stirring period, a deep-yellow solution was formed. Evaporation of toluene gave a deep yellow oil. The crude product was purified by column chromatography on silica gel with petroleum ether/ethyl acetate mixture (200 : 1) as an eluent, affording **1b** (9.27 g, 30.0 mmol) as a deep yellow oil in 75.0% yield. ^1H NMR (300 MHz, CDCl_3): δ 11.54 (s, 1H, O–H), 8.29 (d, 1H, Ar), 7.51 (t, 1H, Ar), 8.29 (d, 1H, Ar), 7.36–7.28 (m, 4H, Ar), 7.08 (t, 1H, Ar), 6.82 (d, 2H, Ar), 6.51 (s, 1H, =CH). ^{13}C NMR (75 MHz, CDCl_3): δ 187.46, 159.84, 147.62, 136.54, 132.52, 129.49, 127.98, 125.30, 124.97, 123.41, 120.86, 117.17, 115.54, 94.98. Anal. Calcd. for $\text{C}_{16}\text{H}_{11}\text{F}_4\text{NO}$: C, 62.14; H, 3.59; N, 4.53; Found: C, 62.28; H, 3.64; N, 4.49. Complexes **1c–t** were prepared *via* a procedure similar to that for **2b**, the ^1H NMR and the ^{13}C NMR of these obtained complexes were available in the ESI.†

Titanium complexes synthesis.

$[\text{PhN}=\text{C}(\text{CF}_3)\text{CHC}(o\text{-FPh})\text{O}]_2\text{TiCl}_2$ (**2b**)

To a stirred solution of compound $\text{PhN}=\text{C}(\text{CF}_3)\text{CHC}(o\text{-FPh})\text{OH}$ (**1b**, 1.24 g, 4 mmol) in dried diethyl ether (20 mL) at -78 °C, a 1.6 M *n*-butyllithium hexane solution (2.5 mL, 4 mmol) was added dropwise over 5 min. The mixture was allowed to warm to room temperature and stirred for 2.5 h. Then, the mixture was added dropwise to TiCl_4 (2 mmol) in dried diethyl ether (30 mL) at -78 °C with stirring over 30 min. The mixture was allowed to warm to room temperature and stirred overnight. The evaporation of the solvent in vacuum yielded a crude product. Dried CH_2Cl_2 and *n*-hexane were added to the solid residue, and the mixture was stirred for 10 min. The filtration of the mixture gave complex **2b** as a red solid in 61% yield. ^1H NMR (300 MHz, CDCl_3): δ 7.70 (td, 2H, Ar–H), 7.46 (q, 2H, Ar–H), 7.29 (t, 2H, Ar–H), 7.20–7.04 (m, 6H, Ar–H), 6.92 (t, 2H, Ar–H), 6.81–6.78 (m, 6H, Ar–H and =CH). Anal. Calcd. for $\text{C}_{32}\text{H}_{20}\text{Cl}_2\text{F}_8\text{N}_2\text{O}_2\text{Ti}$: C, 52.27; H, 2.74; N, 3.81; Found: C, 52.18; H, 2.69; N, 3.86. Complexes **2c–2t** were prepared *via* a procedure similar to that for **2b**, the ^1H NMR and the ^{13}C NMR of these obtained complexes were available in the ESI.†

X-Ray crystallography†

Single crystals of complexes **2h**, **2k**, **2m**, **2n** and **2s** suitable for X-ray structure determination were grown from dichloromethane–hexane solution at room temperature in a glove box, thus maintaining a dry, O_2 -free environment. The X-ray diffraction data of the complexes were collected on a Bruker Smart CCD diffractometer equipped with graphite monochromated $\text{Mo-K}\alpha$ radiation ($\lambda = 0.71073$ Å) at 187 K. Empirical absorption corrections were applied to the data using the SADABS program. The structures were solved by the direct method and refined by the full-matrix least-squares on F^2 using the SHELXTL-97 program.^{31–32} All of

the non-hydrogen atoms were refined anisotropically. Crystallographic data and other pertinent information for the complexes are summarized in Table 1. Selected bond lengths and angles are listed in Table 2.

Ethylene polymerization

Polymerization was carried out under atmospheric pressure in toluene in a 150 ml glass reactor equipped with a mechanical stirrer. Toluene (50 mL) was introduced into the argon-purged reactor and stirred vigorously (600 rpm). The toluene was kept at a prescribed polymerization temperature, and then the ethylene gas feed was started. After 15 min, the polymerization was initiated by the addition of a heptane solution of MMAO and a toluene solution of one of the titanium complexes into the reactor with vigorous stirring (600 rpm). After a prescribed time, isobutyl alcohol (10 mL) was added to terminate the polymerization reaction, and the ethylene gas feed was stopped. The resulted mixture was added to the acidic methanol (1 mL concentrated of HCl in 500 mL of methanol). The solid polyethylene was isolated by filtration, washed with methanol, and dried at 60 °C for 24 h in a vacuum oven.

Ethylene/norbornene copolymerization

The copolymerization was performed in a glass flask (150 mL) equipped with a mechanical stirrer. Toluene (50 mL) was introduced to the argon-purged reactor and stirred at 600 rpm. The solvent was kept at the prescribed polymerization temperature, and then the prescribed amount of norbornene was charged into the reactor. The ethylene gas feed was started. After 15 min, polymerization was initiated by the addition of a MMAO heptane solution and then a solution of titanium complexes in toluene into the reactor. The polymerization was quenched after the prescribed time by the addition of isobutyl alcohol (5 mL). The resulting mixture was added to the acidic methanol. The copolymer was collected by filtration, washed with methanol, and then dried at 60 °C for 24 h in a vacuum.

Acknowledgements

The authors are grateful for the support of the National Natural Science Foundation of China (Nos. 20734002 and 20874096), and by the Special Funds for Major State Basis Research Projects (No. 2005CB623800) from the Ministry of Science and Technology of China.

References

- 1 For reviews see: S. D. Ittel, L. K. Johnson and M. Brookhart, *Chem. Rev.*, 2000, **100**, 1169; G. W. Coates, P. D. Hustad and S. Reinartz, *Angew. Chem., Int. Ed.*, 2002, **41**, 2236; V. C. Gibson and S. K. Stefan, *Chem. Rev.*, 2003, **103**, 283; G. J. Domsikia, J. M. Rose, G. W. Coates, A. D. Bolig and M. Brookhart, *Prog. Polym. Sci.*, 2007, **32**, 30; T. Matsugi and T. Fujita, *Chem. Soc. Rev.*, 2008, **37**, 1264; H. Makio and T. Fujita, *Acc. Chem. Res.*, 2009, **42**, 1532.
- 2 D. W. Stephan, J. C. Stewart, F. Guérin, R. E. v. H. Spence, W. Xu and D. G. Harrison, *Organometallics*, 1999, **18**, 1116; O. Alhomainan, C. Beddie, G. Bai and D. W. Stephan, *Dalton Trans.*, 2009, 1991; K. Yadav, J. S. J. McCahill, G. Bai and D. W. Stephan, *Dalton Trans.*, 2009, 1636.
- 3 J. Niemeyer, G. Kehr, R. Frölich and G. Erker, *Chem.–Eur. J.*, 2008, **14**, 9499; J. Niemeyer, G. Kehr, R. Frölich and G. Erker, *Dalton Trans.*, 2009, 3731.
- 4 F. Gornshstein, M. Kapon, M. Botoshansky and M. S. Eisen, *Organometallics*, 2007, **26**, 497; P. Elo, A. Parssinen, M. Nieger, M. Leskela and T. Repo, *J. Organomet. Chem.*, 2009, **694**, 2927.
- 5 R. J. Long, V. C. Gibson, A. J. P. White and D. J. Williams, *Inorg. Chem.*, 2006, **45**, 511; R. J. Long, V. C. Gibson and A. J. P. White, *Organometallics*, 2008, **27**, 235; R. J. Long, D. J. Jones, V. C. Gibson and A. J. P. White, *Organometallics*, 2008, **27**, 5960; L. P. He, J. Y. Liu, Y. G. Li, S. R. Liu and Y. S. Li, *Macromolecules*, 2009, **42**, 8566.
- 6 L. Annunziata, D. Pappalardo, C. Tedesco and C. Pellecchia, *Macromolecules*, 2009, **42**, 5572; L. Annunziata, D. Pappalardo, C. Tedesco and C. Pellecchia, *Organometallics*, 2009, **28**, 688.
- 7 V. Volkis, M. Rodensky, A. Lisovskii, Y. Balazs and M. S. Eisen, *Organometallics*, 2006, **25**, 4934; F. Chen, M. Kapon, J. D. Woollins and M. S. Eisen, *Organometallics*, 2009, **28**, 2391.
- 8 B. Lian, K. Beckerle, T. P. Spaniol and J. Okuda, *Eur. J. Inorg. Chem.*, 2009, 311; K. Itagaki, K. Kakinuki, S. Katao, T. Khamnaen, M. Fujiki, K. Nomura and S. Hasumi, *Organometallics*, 2009, **28**, 1942; K. H. Tam, M. C. W. Chan, H. Kaneyoshi, H. Makio and N. Y. Zhu, *Organometallics*, 2009, **28**, 5877; Y. B. Huang, W. B. Yu and G. X. Jin, *Organometallics*, 2009, **28**, 4170; X. H. Yang, Z. Wang, X. L. Sun and Y. Tang, *Dalton Trans.*, 2009, 8945.
- 9 S. J. Luo, J. Vela, G. R. Lief and R. F. Jordan, *J. Am. Chem. Soc.*, 2007, **129**, 8946; D. Guironnet, P. Roesle, T. Rünzi, I. Göttker-Schnetmann and S. Mecking, *J. Am. Chem. Soc.*, 2009, **131**, 422; S. Ito, K. Munakata, A. Nakamura and K. Nozaki, *J. Am. Chem. Soc.*, 2009, **131**, 14606.
- 10 J. D. Azoulay, K. Itigaki, G. Wu and G. C. Bazan, *Organometallics*, 2008, **27**, 2273; S. J. Diamanti, V. Khanna, A. Hotta, D. Yamakawa, F. Shimizu, E. J. Kramer, G. H. Fredrickson and G. C. Bazan, *J. Am. Chem. Soc.*, 2004, **126**, 10528.
- 11 C. S. Popeney, D. H. Camacho and Z. Guan, *J. Am. Chem. Soc.*, 2007, **129**, 10062; D. H. Camacho and Z. Guan, *Macromolecules*, 2005, **38**, 2544; D. H. Leung, J. W. Ziller and Z. Guan, *J. Am. Chem. Soc.*, 2008, **130**, 7538.
- 12 M. A. Zuideveld, P. Wehrmann, C. Rohr and S. Mecking, *Angew. Chem., Int. Ed.*, 2004, **43**, 869; D. Guironnet, T. Friedberger and S. Mecking, *Dalton Trans.*, 2009, 8929.
- 13 S. Sujith, D. J. Joe, S. J. Na, Y. W. Park, C. H. Choi and B. Y. Lee, *Macromolecules*, 2005, **38**, 10027; B. A. Rodriguez, M. Delferro and T. J. Marks, *J. Am. Chem. Soc.*, 2009, **131**, 5902; B. A. Rodriguez, M. Delferro and T. J. Marks, *Organometallics*, 2008, **27**, 2166.
- 14 J. D. Azoulay, R. S. Rojas, A. V. Serrano, H. Ohtaki, G. B. Galland, G. Wu and G. C. Bazan, *Angew. Chem., Int. Ed.*, 2008, **47**, 1; J. D. Azoulay, Y. Schneider, G. B. Galland and G. C. Bazan, *Chem. Commun.*, 2009, 6177.
- 15 M. Mitani, J. Mohri, Y. Yoshida, J. Saito, S. Ishii, K. Tsuru, S. Matsui, R. Furuyama, T. Nakano, H. Tanaka, S. I. Kojoh, T. Matsugi, N. Kashiwa and T. Fujita, *J. Am. Chem. Soc.*, 2002, **124**, 3327; M. Mitani, R. Furuyama, J. Mohri, J. Saito, S. Ishii, H. Terao, N. Kashiwa and T. Fujita, *J. Am. Chem. Soc.*, 2002, **124**, 7888; M. Mitani, R. Furuyama, J. Mohri, J. Saito, S. Ishii, H. Terao, T. Nakano, H. Tanaka and T. Fujita, *J. Am. Chem. Soc.*, 2003, **125**, 4293.
- 16 P. D. Hustad and G. W. Coates, *J. Am. Chem. Soc.*, 2002, **124**, 11578; A. F. Mason, J. Tian, P. D. Hustad, E. B. Lobkovsky and G. W. Coates, *Isr. J. Chem.*, 2002, **42**, 301; A. F. Mason and G. W. Coates, *J. Am. Chem. Soc.*, 2004, **126**, 10798; A. F. Mason and G. W. Coates, *J. Am. Chem. Soc.*, 2004, **126**, 16326.
- 17 M. Lamberti, D. Pappalardo, A. Zambelli and C. Pellecchia, *Macromolecules*, 2002, **35**, 658.
- 18 S. Reinartz, A. F. Mason, E. B. Lobkovsky and G. W. Coates, *Organometallics*, 2003, **22**, 2542.
- 19 X. F. Li, K. Dai, W. P. Ye, L. Pan and Y. S. Li, *Organometallics*, 2004, **23**, 1223.
- 20 L. M. Tang, T. Hu, Y. J. Bo, Y. S. Li and N. H. Hu, *J. Organomet. Chem.*, 2005, **690**, 3135.
- 21 W. P. Ye, J. Zhan, L. Pan, N. H. Hu and Y. S. Li, *Organometallics*, 2008, **27**, 3642.
- 22 W. P. Ye, H. L. Mu, X. C. Shi, Y. X. Cheng and Y. S. Li, *Dalton Trans.*, 2009, 9452.
- 23 L. M. Tang, Y. Q. Duan and Y. S. Li, *J. Polym. Sci., Part A: Polym. Chem.*, 2005, **43**, 1681; L. M. Tang, T. Hu, L. Pan and Y. S. Li, *J. Polym. Sci., Part A: Polym. Chem.*, 2005, **43**, 6323; L. Pan, W. P. Ye, J. Y. Liu, M. Hong and Y. S. Li, *Macromolecules*, 2008, **41**, 2981; L. Pan, M. Hong, J. Y. Liu, W. P. Ye and Y. S. Li, *Macromolecules*, 2009, **42**, 4391; J. Y. Liu, S. R. Liu, L. Pan and Y. S. Li, *Adv. Synth. Catal.*, 2009, **351**, 1505.

- 24 S. M. Yu and S. Mecking, *J. Am. Chem. Soc.*, 2008, **130**, 13204; S. G. Gong, H. Y. Ma and J. L. Huang, *Dalton Trans.*, 2009, 8237; G. Y. Xie, Y. X. Li, J. Sun and C. T. Qian, *Inorg. Chem. Commun.*, 2009, **12**, 796; X. H. Yang, X. L. Sun, F. B. Han, B. Liu, Y. Tang, Z. Wang, M. L. Gao, Z. W. Xie and S. Z. Bu, *Organometallics*, 2008, **27**, 4618.
- 25 C. Nájera, J. M. Sansano and M. Yus, *Tetrahedron*, 2003, **59**, 9255.
- 26 K. J. MacNeil and D. J. Burton, *J. Org. Chem.*, 1993, **58**, 4411.
- 27 Z. D. Tomić, V. M. Leovac, Ž. K. Jaćimović, G. Giester and S. D. Zarić, *Inorg. Chem. Commun.*, 2006, **9**, 833; A. Kermagoret and P. Braunstein, *Dalton Trans.*, 2008, 822.
- 28 K. Vanka, Z. Xu and T. Ziegler, *Organometallics*, 2004, **23**, 2900.
- 29 R. T. Morison, R. M. Boyd Ed. *Organic Chemistry*, 4th ed.; Allyn and Bacon, Inc., Boston, 1983, pp 614-620.
- 30 Y. Yoshida, J. Mohri, S. Ishii, M. Mitani, J. Saito, S. Matsui, H. Makio, T. Nakano, H. Tanaka, M. Onda, Y. Yamamoto, A. Mizuno and T. Fujita, *J. Am. Chem. Soc.*, 2004, **126**, 12023.
- 31 Siemens. *ASTRO, SAINT and SADABS. Data Collection and Processing Software for the SMART System*, Siemens Analytical X-ray Instruments Inc., Madison, WI, 1996.
- 32 G. M. Sheldrick, *SHELXL-97, A Program for Crystal Structure Refinement*, University of Göttingen: Göttingen, Germany, 1997.